Am J Transl Res 2025;17(8):6370-6380
www.ajtr.org /ISSN:1943-8141/AJTR0166035

Original Article

A combined clinical-ultrasound radiomics model for differentiating benign and malignant BI-RADS category 4 breast masses

Qing Zhang[1*], Juan Gao[1*], Enock Adjei Agyekum[2], Linna Zhu[1], Chao Jiang[3], Suping Du[4], Liang Yin[5]

[1]Department of Ultrasound, Jiangsu University Affiliated People's Hospital, Zhenjiang, Jiangsu, China; [2]School of Medicine, Jiangsu University, Zhenjiang, Jiangsu, China; [3]Department of Orthopedics, Jiangsu University Affiliated Hospital, Zhenjiang, Jiangsu, China; [4]Department of Dermatology, Jiangsu University Affiliated People's Hospital, Zhenjiang, Jiangsu, China; [5]Department of Breast Surgery, Jiangsu University Affiliated People's Hospital, Zhenjiang, Jiangsu, China. [*]Equal contributors.

Received May 14, 2025; Accepted July 5, 2025; Epub August 15, 2025; Published August 30, 2025

Abstract: Purpose: To evaluate the diagnostic performance of a model combining gray-scale ultrasound (US) radiomic features and clinical data in distinguishing benign from malignant breast masses classified as Breast Imaging Reporting and Data System (BI-RADS) category 4. Methods: In this retrospective study, 149 women with pathologically confirmed breast masses were included and randomly divided into a training cohort (n=104) and a validation cohort (n=45). A total of 1,046 radiomic features were extracted from US images. Feature selection was performed using Pearson correlation analysis followed by least absolute shrinkage and selection operator (LASSO) regression. Three K-nearest neighbor (KNN) classifiers were developed: a clinical model, an ultrasound radiomics (USR) model, and a combined clinical-USR model. Model performance was assessed using accuracy, sensitivity, specificity, and the area under the receiver operating characteristic curve (AUC). Results: Seven radiomic features and two clinical variables were selected for model construction. In the training cohort, the combined clinical-USR model achieved an AUC of 0.927, with an accuracy of 89.0%, sensitivity of 88.9%, and specificity of 89.8%. In the validation cohort, the AUC of 0.826, with an accuracy of 80.0%, sensitivity of 83.3%, and specificity of 66.7%. The standalone USR model yielded AUCs of 0.902 and 0.883 in the training and validation cohorts, respectively, while the clinical model showed lower AUCs of 0.876 and 0.794. Decision curve analysis (DCA) indicated that the combined model provided a greater net clinical benefit than the clinical model alone. Conclusion: The integration of ultrasound radiomic features with clinical data improves diagnostic performance in differentiating benign from malignant BI-RADS 4 breast masses. The combined model holds potential for aiding clinical decision-making but requires further validation in larger, independent datasets.

Keywords: Ultrasound radiomics, clinical data integration, breast masses, BI-RADS 4, machine learning, diagnostic imaging

Introduction

Breast cancer remains the most commonly diagnosed malignant tumor among women worldwide and is a leading cause of cancer-related deaths, posing a significant challenge to public health [1]. Timely and accurate diagnosis is critical for improving patient prognosis, and imaging plays a pivotal role in the clinical management of breast cancer, including screening, diagnosis, staging, treatment planning, and monitoring therapeutic response [2].

Among the various imaging modalities, ultrasound (US) is widely utilized due to its real-time imaging capabilities, lack of ionizing radiation, affordability, and accessibility - especially in resource-limited settings [3-5]. It is particularly valuable for evaluating palpable breast abnormalities, guiding biopsies, and characterizing masses in dense breast tissue where mammography may be less effective.

To standardize breast imaging interpretation and improve communication among healthcare providers, the American College of Radiology

https://doi.org/10.62347/SBKU2090

(ACR) developed the Breast Imaging Reporting and Data System (BI-RADS). The BI-RADS ultrasound lexicon classifies breast lesions based on specific sonographic features. Category 4 lesions are considered "suspicious for malignancy", with a broad malignancy probability ranging from 2% to 95%. To refine risk stratification and guide clinical management, BI-RADS 4 is further divided into three subcategories: 4A (low suspicion, 2%-10%), 4B (moderate suspicion, 10%-50%), and 4C (high suspicion, 50%-95%) [6]. Despite this stratification, BI-RADS 4 lesions typically require tissue sampling, which often results in a high number of unnecessary biopsies, particularly for lesions in the lower-risk subcategories.

Accurate BI-RADS classification relies heavily on the radiologist's subjective interpretation of morphological features, which may vary depending on individual experience and training. Studies have shown considerable inter-observer variability in BI-RADS assessments, particularly within category 4 [7-11]. Additionally, the substantial overlap in ultrasound characteristics between benign and malignant masses further complicates accurate differentiation. Although clinical factors-such as patient age, lesion palpability, and personal or family history of breast cancer, can aid in risk assessment, these are not consistently incorporated into routine ultrasound evaluations.

Recent advancements in medical imaging analysis have introduced radiomics as a powerful approach to extract high-dimensional quantitative features from standard medical images. These features capture tissue characteristics - such as heterogeneity, texture, and morphology - that are often imperceptible to the human eye but may be indicative of malignancy [12]. The integration of radiomics with machine learning has shown promising results in various oncologic imaging applications. However, its application in ultrasound imaging, especially for evaluating BI-RADS 4 breast lesions, remains relatively underexplored. Given the need for more objective and reproducible diagnostic tools, this study aims to develop and evaluate machine learning models that integrate grayscale ultrasound-based radiomic features with clinical data to differentiate between benign and malignant BI-RADS category 4 breast masses. The ultimate goal is to improve diagnostic accuracy, reduce unnecessary biopsies, and support more personalized patient care.

Materials and methods

Study design and patient selection

This retrospective study was approved by the Ethics Committee of the Affiliated People's Hospital of Jiangsu University (Approval No. SQK-20230061-W). Owing to the retrospective nature of the study, the requirement for written informed consent was waived.

Between September 2021 and April 2022, 149 consecutive female patients who underwent ultrasound-guided core needle biopsy (US-CNB) or surgical excision for breast masses were evaluated. All patients had undergone standardized preoperative breast ultrasound (US) examinations. After applying specific eligibility criteria, a total of 149 breast lesions from 149 women were included in the final analysis. The patients' ages ranged from 23 to 77 years, with a mean of 53.75±11.98 years.

Inclusion criteria were: (1) solid or predominantly solid breast masses confirmed by US; (2) availability of complete clinical, imaging, and pathological data; and (3) no prior treatment, such as chemotherapy or radiotherapy, before the imaging evaluation. Exclusion criteria included: (1) purely cystic lesions; (2) incomplete imaging or pathological data; and (3) poor image quality unsuitable for accurate assessment.

Ultrasound acquisition and BI-RADS classification

All US examinations were performed using a Mindray 7s Imagine ultrasound system (Mindray Medical, Shenzhen, China) equipped with a 5-14 MHz linear-array transducer. Two radiologists, each with 5 to 15 years of experience in breast ultrasound, conducted the examinations. They had access to the patients' clinical information at the time of scanning.

During the examinations, Patients were positioned supine with arms raised to ensure full exposure of breast tissue. Both transverse and longitudinal images of each lesion were acquired. For each lesion, Sonographic features evaluated included echogenicity, shape, orientation, margins, posterior acoustic features, presence of calcifications, vascularity, and tissue elasticity. A representative high-quality image with minimal artifacts and without measurable markers were selected for further analysis.

The BI-RADS system developed by the American College of Radiology (ACR) standardizes terminology, reporting formats, examination techniques, and diagnostic procedures of breast imaging to facilitate clinical decision-making and interprofessional communication. BI-RADS has been widely adopted in clinical breast ultrasound practice in China. Lesions exhibiting three or more suspicious features - such as irregular shape, non-parallel orientation, non-circumscribed margin, posterior shadowing, a hyperechoic halo, surrounding tissue distortion, microcalcifications (less than 0.5 mm), or intralesional vascularity - were categorized as BI-RADS 5. Lesions with a regular shape, a circumscribed margin, and parallel orientation were categorized as BI-RADS 3. Lesions not clearly fitting either category were assigned to BI-RADS subcategories 4A, 4B, or 4C, based on the degree and number of suspicious features.

Image segmentation and radiomic feature extraction

For each lesion, a representative US image was selected, and the region of interest (ROI) was manually delineated along the lesion boundary using ITK-SNAP software (version 3.8.0; http://www.itksnap.org). ROI segmentation was independently performed by two radiologists with 15 and 10 years of experience, respectively. Discrepancies were resolved by consensus to ensure consistency.

A total of 1,046 quantitative radiomic features were extracted from each ROI using the open-source Pyradiomics package (version 2.2.0; https://github.com/Radiomics/pyradiomics). Extracted features included first-order statistics, shape-based descriptors, and a range of texture features derived from gray-level co-occurrence, run-length, size zone, dependence, and neighborhood graytone difference matrices. Additionally, wavelet-transformed versions of each feature category were computed to capture multi-scale texture characteristics.

Feature selection and model construction

To reduce dimensionality and prevent overfitting, radiomic features were first normalized using a robust scaler. Features with high redundancy (Pearson correlation coefficients > 0.80) were removed, prioritizing retention of original, low-order features. Feature selection was then performed using least absolute shrinkage and selection operator (LASSO) regression with 10-fold cross-validation to identify the most predictive features.

A k-nearest neighbor (KNN) classifier was trained using the selected radiomic features to build the Ultrasound Radiomics (USR) model. The diagnostic performance of this model was evaluated on both training and validation datasets based on receiver operating characteristic (ROC) curve analysis, sensitivity, specificity, accuracy, positive predictive value (PPV), and negative predictive value (NPV).

In addition to the USR model, a Clinical Model was developed using statistically significant clinical variables and conventional sonographic features identified through univariate analysis. Finally, a combined Clinical-USR Model was constructed by integrating clinical data, imaging characteristics, and selected radiomic features. All models were built using the same KNN classification algorithm, and their performances were compared in both training and validation cohorts to evaluate the added diagnostic value of incorporating radiomics data.

Statistical analysis

The Kolmogorov-Smirnov test was used to assess the normality of all continuous variables, and the F-test was applied to evaluate the homogeneity of variance. All continuous variables included in this study met the assumptions for normality and homogeneity of variance. Continuous variables were expressed as mean ± standard deviation (SD), and between-group differences were analyzed using the independent samples t-test. Categorical variables were presented as frequency and percentages, with group comparisons performed using the Chi-square test. Univariate logistic regression analysis was conducted to identify potential risk factors. Variables with a P value <0.05 in the univariate analysis were included in the multivariate logistic regression mode to determine independent risk factors. Receiver operating characteristic (ROC) curve analysis and the area under the curve (AUC) were used to assess the discriminatory ability of the model. In addition, a calibration curve was used to assess agreement between predicted and observed outcomes, and decision curve analysis (DCA) was performed to evaluate the clinical value of the predictive model. All statistical analyses were performed using Python (version 3.7), IBM SPSS Statistics for Windows (version

Table 1. Patient characteristics of the training and validation cohorts

Characteristic	Training Cohort (104)	Validation Cohort (45)	*P* value	X^2/t
Age, mean ± SD (year)	52.75±11.32	55.48±13.00	0.000*	-8.528
Tumor size (mm)	25.23±11.99	30.99±18.06	0.06	-10.515
Menopause history			0.709	0.14
Menopause	52	24		
Premenopausal	52	21		
Tumor location			0.444	0.586
Left breast	53	26		
Right breast	51	19		
Tumor position			0.06	5.628
Outer upper quadrant	93	35		
Outer lower quadrant	8	4		
Inner upper quadrant	3	6		
Inner lower quadrant	0	0		
Internal echo			0.734	0.693
Hypoecho	98	43		
Hyper echo	1	0		
Iso echo	0	0		
Mixed echo	5	2		
Tumor margin			0.842	0.04
Circumscribed	49	22		
Not circumscribed	55	23		
Tumor shape			0.527	0.401
Regular	45	22		
Irregular	59	23		
Orientation way			0.023	5.197
Parallel orientation	95	35		
Not Parallel orientation	9	10		
Tumor inner calcification			0.409	2.892
Microcalcification	26	15		
Coarse calcification	11	7		
Mixed calcification	1	1		
Without calcification	66	22		
Tumor vascularization			0.102	4.569
Without	42	10		
A few	26	15		
Abundant	36	20		
Strain elastography			0.065	3.403
Soft	80	28		
Hard	24	17		

*: It means the *P* value is less than 0.05.

26.0; IBM Corp., Armonk, NY, USA), and the scikit-learn library (version 1.2). A *P* value <0.05 was considered statistically significant.

Results

Patient characteristics and cohort allocation

A total of 149 female patients were enrolled in this study, comprising 71 individuals with histopathologically confirmed benign breast lesions and 78 with malignant lesions. The overall mean age was 53.75±11.98 years, ranging from 23 to 77 years (**Table 1**). Patients were randomly assigned to either a training cohort (n=104) or a validation cohort (n=45) using stratified random sampling to maintain a balanced distribution of benign and malignant cases across both groups.

Table 2. Patient characteristics of the benign and malignant breast masses

Characteristic	Benign (n=71)	Malignant (n=78)	*P* value	X^2/t
Age, mean ± SD (year)	46.37±11.49	54.81±11.70	0.000*	-4.437
Tumor size (mm)	17.42±12.37	23.06±9.81	0.002*	-3.097
Menopause history			0.001*	11.234
menopause	26	50		
premenopausal	45	28		
Tumor location			0.656	0.199
left breast	39	40		
right breast	32	38		
Tumor position			0.640	0.891
outer upper quadrant	61	68		
outer lower quadrant	7	5		
inner upper quadrant	3	5		
inner lower quadrant	0	0		
Internal echo			0.794	0.068
hypoecho	68	74		
hyperecho	0	0		
isoecho	0	0		
mixed echo	3	4		
Tumor margin			0.000*	12.238
circumscribed	44	26		
non-circumscribed	27	52		
Tumor shape			0.018*	5.643
regular	19	9		
irregular	52	69		
Orientation way			0.339	0.916
Parallel orientation	60	70		
Not Parallel orientation	11	8		
Tumor inner calcification			0.000*	39.079
Microcalcification	7	34		
Coarse calcification	17	1		
Mixed calcification	2	0		
Without calcification	45	43		
Tumor vascularization			0.063	5.527
Without	27	25		
A few	24	17		
Abundant	20	36		
Strain elastography			0.000*	51.137
Soft	69	32		
Hard	2	46		

*: It means the *P* value is less than 0.05.

Baseline clinical and imaging features were compared between the benign and malignant groups. Statistically significant differences were observed in patient age, the presence of internal calcifications, and strain elastography results ($P<0.05$ for all). These variables were considered relevant and included in the development of the Clinical Model (**Table 2**).

Performance of the clinical prediction model

The Clinical Model was developed using three variables - age, internal calcification, and strain elastography - that showed significant differences between benign and malignant lesions. Feature selection was performed using LASSO regression to reduce dimensionality and avoid

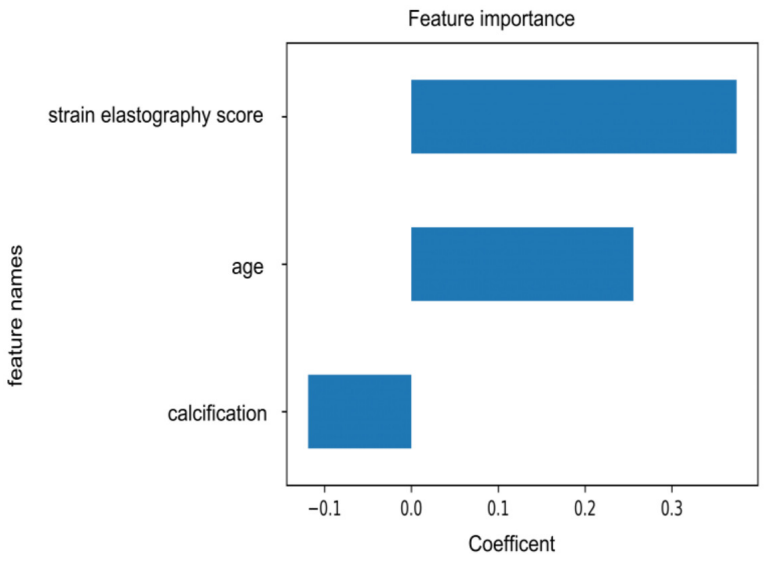

Figure 1. Feature selection process for the clinical model. This figure illustrates the dimensionality reduction process for clinical variables in the training cohort. Following statistical analysis and feature selection, three clinical features with significant discriminative power in distinguishing benign from malignant breast lesions were retained for model construction.

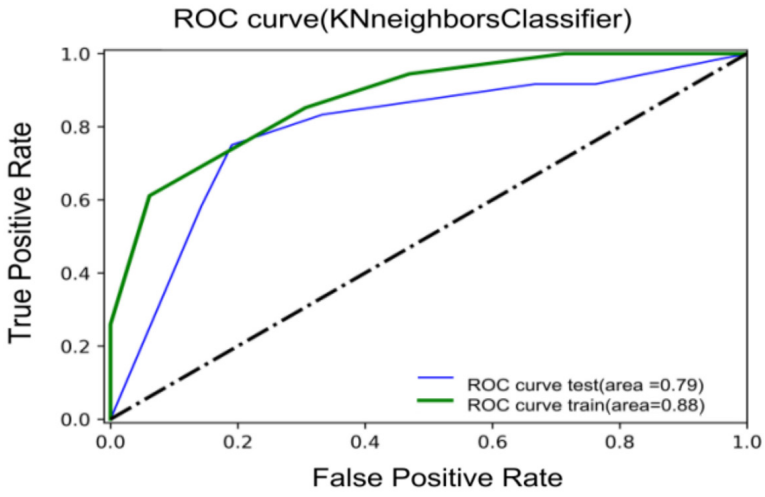

Figure 2. Receiver operating characteristic (ROC) curves for the clinical model. ROC curves for both the training and validation cohorts are presented to evaluate the diagnostic performance of the Clinical model. The curves reflect the model's ability to differentiate between benign and malignant lesions based on selected clinical features. The AUC was 0.88 in the training cohort and 0.79 in the validation cohort.

overfitting (**Figure 1**). The model was trained using the KNN algorithm. In the training cohort, the Clinical Model achieved an AUC of 0.876, indicating good discrimination between benign and malignant lesions. In the validation cohort, the model demonstrated acceptable performance with an AUC of 0.794 (**Figure 2**).

Construction and evaluation of the USR model

From the initial set of 1,046 radiomic features extracted from ultrasound images, 15 were selected via LASSO regression based on the training dataset. These features were used to build the USR Model using a KNN classifier (**Figure 3**). The USR Model demonstrated strong diagnostic performance, achieving an AUC of 0.902 in the training cohort. In the validation cohort, the model maintained excellent performance, with an AUC of 0.883 (**Figure 4**), suggesting robust generalizability of the radiomics-based approach.

Development and performance of the combined clinical-USR model

To evaluate the added value of integrating clinical and radiomic data, a combined Clinical-USR Model was developed. This model incorporated the three clinical variables along with the selected radiomic features. Redundant features were eliminated using Pearson correlation coefficient analysis, and LASSO regression with cross-validation was applied to finalize feature selection (**Figure 5**). A total of 15 combined features were used to construct the model.

The final predictive model was developed using the KNN classifier (**Figure 6**). In the training cohort, the Clinical-USR Model achieved the highest AUC of 0.927, with a sensitivity of 0.889 and specificity of 0.898. In the validation cohort, the model retained good performance, achieving an AUC of 0.826, with sensitivity and specificity of 0.833 and 0.667, respectively.

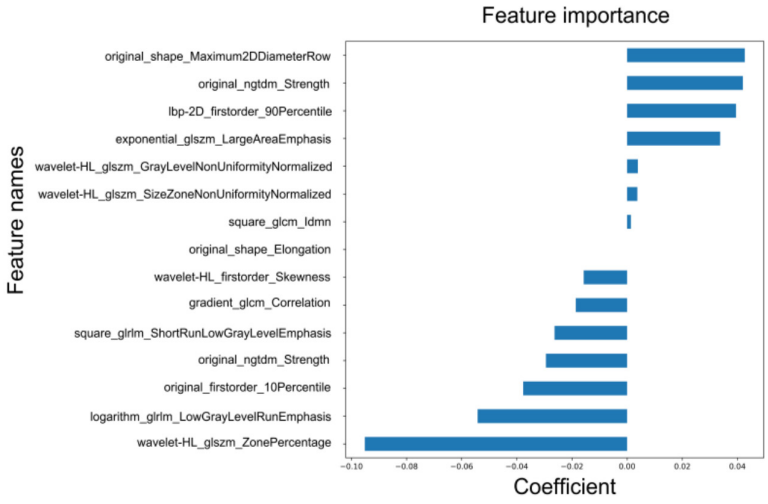

Figure 3. Feature selection process for the ultrasound radiomics (USR) model. This figure depicts the feature selection process for radiomic features extracted from grayscale ultrasound images in the training cohort. Out of 1,046 initially extracted features, 15 were selected using Pearson correlation analysis followed by LASSO regression for input into the USR model.

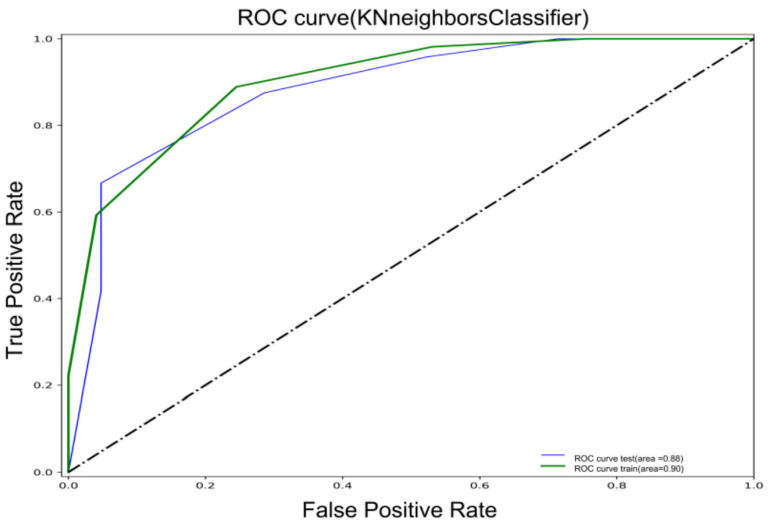

Figure 4. Receiver operating characteristic (ROC) curves for the USR model. ROC curves for the training and validation cohorts are shown to assess the diagnostic performance of the USR model. The curves demonstrate strong discriminatory power of the selected radiomic features in classifying BI-RADS 4 breast lesions. The AUC was 0.90 in the training cohort and 0.88 in the validation cohort.

Comparative analysis of the model performance

A comparative analysis of the three models - Clinical, USR, and Clinical-USR - was conducted to evaluate diagnostic performance (**Table 3**).

• In the training cohort, the Clinical-USR Model showed the highest AUC (0.927), followed by the USR Model (0.902) and the Clinical Model (0.876).

• In the validation cohort, the USR Model achieved the highest AUC (0.883), outperforming the Clinical-USR (0.826) and Clinical Models (0.794).

• Although the Clinical-USR Model showed slightly lower performance than the USR Model in the validation cohort, it exhibited improved sensitivity over the Clinical Model.

Consistent classification thresholds were used across cohorts: 0.800 for the Clinical Model, and 0.600 for both the USR and Clinical-USR Models.

Decision curve analysis (DCA) demonstrated that the Clinical-USR model provided a greater net benefit compared to clinical model across threshold probabilities ranging from 20% to 45%. The maximum net benefit (0.28) was observed at a threshold probability of 30%, suggesting that the Clinical-USR model would offer a clinically meaningful improvement in decision-making over the Clinical Model alone.

Discussion

In recent years, advancements in ultrasound imaging technology - including higher-resolution probes and improved imaging techniques - have significantly enhanced the early detection and diagnosis of breast cancer. Among non-invasive imaging modalities, grayscale ultrasound remains a first-line tool for screening and diagnosing breast lesions due to its accessibility, cost-effectiveness, and real-time capabilities [13, 14]. However, conventional ultrasound interpretation remains largely qualitative and subjective, relying heavily on radiologists' experience and visual assessment based on the ACR BI-RADS-US lexicon.

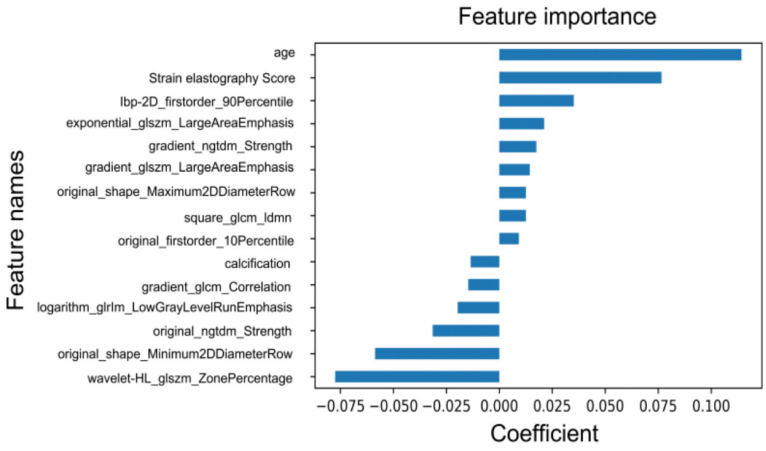

Figure 5. Feature selection process for the combined clinical-USR model. This figure illustrates the integration and feature selection process for the combined model, incorporating both clinical and radiomic variables. A total of 15 features - comprising 3 clinical and 12 radiomic features - were retained in the training cohort following comprehensive selection procedures to construct the integrated model.

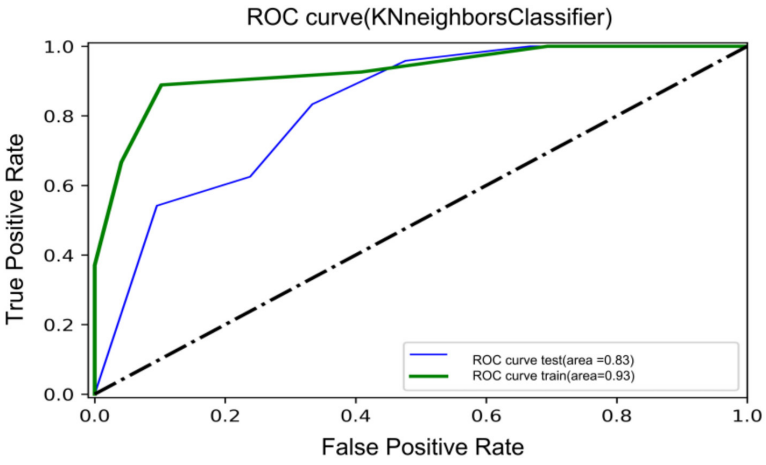

Figure 6. Receiver operating characteristic (ROC) curves for the combined clinical-USR model. ROC curves for the training and validation cohorts demonstrate the enhanced diagnostic performance of the combined Clinical-USR Model. The integrated model outperformed the individual Clinical or USR models, highlighting its potential clinical value in differentiating benign from malignant BI-RADS 4 lesions. The AUC was 0.93 in the training cohort and 0.83 in the validation cohort.

The BI-RADS 4 category presents a particular diagnostic challenge due to its broad range of malignancy probability (5-90%) [15], leading to high variability in diagnostic outcomes. In our study, 48% of BI-RADS 4 lesions were ultimately diagnosed as benign based on pathology, highlighting the limitations of visual assessment and the potential for both overtreatment and delayed diagnosis. False-negative cases - where malignant tumors with subtle ultrasound features are misclassified - may delay timely treatment, while False-positive cases can result in unnecessary biopsies and increased psychological burden. These challenges underscore the need for adjunctive, objective tools to improve the risk stratification of BI-RADS 4 lesions.

Radiomics enables the extraction of high-throughput, quantitative features from medical images, capturing tissue characteristics that are often imperceptible to the human eye. This approach has shown promise in various malignancies and may aid in clinical decision-making [16-19]. Moreover, combining radiomics with multi-omic approaches - such as radiogenomics - could further enhance predictive models. In this study, we proposed a novel diagnostic method that combines ultrasound radiomics features with clinical data to improve the diagnostic efficiency of breast lesions. The model was developed using a machine learning pipeline based on K-nearest neighbors (KNN) algorithm, with feature selection via Pearson correlation coefficient filtering and LASSO regression.

The Clinical-USR model demonstrated strong discriminatory power, achieving an AUC of 0.927 in the training cohort and 0.826 in the validation cohort. Notably, it outperformed the Clinical model (AUCs: 0.876 and 0.794, respectively). These findings suggest that integrating clinical information with radiomic data yields a more robust predictive framework than either data type alone.

Importantly, the Clinical-USR model surpassed the diagnostic accuracy typically reported for experienced sonographers (AUC range: 0.71-0.79) [20-22], and provided more precise risk stratification than the BI-RADS-US lexicon al-

Table 3. Performance of the constructed radiomic models

Cohort	Model	AUC	SEN	SPE	PPV	NPV	ACC	Cutoff value
Training dataset	Clinical	0.876	0.852	0.694	0.754	0.809	0.777	0.800
	USR	0.902	0.889	0.755	0.800	0.860	0.825	0.600
	Clinical-USR	0.927	0.889	0.898	0.906	0.880	0.89	0.600
Test dataset	Clinical	0.794	0.833	0.667	0.741	0.778	0.756	0.800
	USR	0.883	0.875	0.714	0.778	0.833	0.800	0.800
	Clinical-USR	0.826	0.833	0.667	0.741	0.777	0.755	0.600

one. Our results are comparable to, or slightly better than those from prior studies using mammography or MRI-based radiomics [23-26], and align with recent ultrasound-based machine learning studies [27-29]. Variations in reported AUC values across studies likely reflect differences in sample sizes, lesion characteristics, and imaging protocols. Notably, many previous works have evaluated clinical or radiomic features in isolation [30, 31], whereas our integrated approach addresses a methodological gap and offers a more clinically applicable diagnostic tool.

For less experienced sonographers, this model could assist in decision-making by providing objective, data-driven malignancy risk predictions, which would be especially valuable in resource-limited settings where variability in expertise may affect BI-RADS classification. For more experienced practitioners, the model serves as a valuable complement, enabling deeper quantitative analysis and data-informed risk stratification in challenging or atypical cases. Successful implementation will require explainable AI tools, seamless integration into clinical platforms, and validation of real-world impact through prospective clinical trials. However, integration into fast-paced clinical workflows and achieving real-time diagnostic performance remain ongoing challenges.

Despite the promising results, our study has several limitations. First, it was a retrospective, single-center study with a relatively small sample size, which may limit generalizability. Second, potential selection bias cannot be excluded, as only patients undergoing core biopsy or surgical excision were included. Third, our radiomic analysis was based limited to gray-scale ultrasound images. Future studies should explore the incorporation of additional modalities, such as Doppler or elastography, and conduct multi-center external validation to enhance model robustness and clinical applicability.

Conclusions

In conclusion, we developed a Clinical-USR model that integrates clinical characteristics and ultrasound-based radiomic features for the differential diagnosis of benign and malignant breast lesions. The model demonstrated strong predictive performance and outperformed traditional clinical assessment and BI-RADS-based assessment classification alone. This approach may serve as a valuable adjunct to conventional ultrasound evaluation, particularly in the risk stratification of BI-RADS 4 lesions, potentially reducing unnecessary biopsies and improve the early detection of breast cancer.

Acknowledgements

We acknowledge the work was supported by Jiangsu Province Maternal and Child Health Research Project (F202322) and Zhenjiang Social and Development Project (SH2024091).

Disclosure of conflict of interest

None.

Address correspondence to: Dr. Liang Yin, Department of Breast Surgery, Jiangsu University Affiliated People's Hospital, Zhenjiang, Jiangsu, China. E-mail: njmu0516@163.com; Dr. Suping Du, Department of Dermatology, Jiangsu University Affiliated People's Hospital, Zhenjiang, Jiangsu, China. E-mail: pfkdusuping@163.com; Dr. Chao Jiang, Department of Orthopedics, Jiangsu University Affiliated Hospital, Zhenjiang, Jiangsu, China. E-mail: jiangchaoab@126.com

References

[1] Katsura C, Ogunmwonyi I, Kankam HK and Saha S. Breast cancer: presentation, investigation and management. Br J Hosp Med (Lond) 2022; 83: 1-7.

[2] Balkenende L, Teuwen J and Mann RM. Application of deep learning in breast cancer imaging. Semin Nucl Med 2022; 52: 584-596.

[3] Mutala TM, Mwango GN, Aywak A, Cioni D and Neri E. Determining the elastography strain ratio cut off value for differentiating benign from malignant breast lesions: systematic review and meta-analysis. Cancer Imaging 2022; 22: 12.
[4] Wu J, Ge L, Guo Y, Zhao A, Yao J, Wang Z and Xu D. Predicting hormone receptor status in invasive breast cancer through radiomics analysis of long-axis and short-axis ultrasound planes. Sci Rep 2024; 14: 16503.
[5] Yin L, Wei X, Zhang Q, Xiang L, Zhang Y, Wang D, Chen P, Cao X, Shaibu Z and Qin R. Multimodal ultrasound assessment of mass and non-mass enhancements by MRI: diagnostic accuracy in idiopathic granulomatous mastitis and breast cancer. Breast 2024; 78: 103797.
[6] Eghtedari M, Chong A, Rakow-Penner R and Ojeda-Fournier H. Current status and future of BI-RADS in multimodality imaging, from the AJR Special series on radiology reporting and data systems. AJR Am J Roentgenol 2021; 216: 860-873.
[7] Zheng X, Huang Y, Wang Y, Liu Y, Li F, Han J, Wang J, Cao L and Zhou J. Combination of different types of elastography in downgrading ultrasound breast imaging-reporting and data System category 4a breast lesions. Breast Cancer Res Treat 2019; 174: 423-432.
[8] Zhao C, Xiao M, Liu H, Wang M, Wang H, Zhang J, Jiang Y and Zhu Q. Reducing the number of unnecessary biopsies of US-BI-RADS 4a lesions through a deep learning method for residents-in-training: a cross-sectional study. BMJ Open 2020; 10: e035757.
[9] Gu Y, Tian JW, Ran HT, Ren WD, Chang C, Yuan JJ, Kang CS, Deng YB, Wang H, Luo BM, Guo SL, Zhou Q, Xue ES, Zhan WW, Zhou Q, Li J, Zhou P, Zhang CQ, Chen M, Gu Y, Xu JF, Chen W, Zhang YH, Wang HQ, Li JC, Wang HY and Jiang YX. The utility of the fifth edition of the BI-RADS ultrasound lexicon in category 4 breast lesions: a prospective multicenter study in China. Acad Radiol 2022; 29 Suppl 1: S26-S34.
[10] Wen B, Kong W, Zhang Y, Xue H, Wu M and Wang F. Association between contrast-enhanced ultrasound characteristics and molecular subtypes of breast cancer. J Ultrasound Med 2022; 41: 2019-2031.
[11] Li X, Zhang J, Zhang G, Liu J, Tang C, Chen K, Chen P, Tan L and Guo Y. Contrast-enhanced ultrasound and conventional ultrasound characteristics of breast cancer with different molecular subtypes. Clin Breast Cancer 2024; 24: 204-214.
[12] Scapicchio C, Gabelloni M, Barucci A, Cioni D, Saba L and Neri E. A deep look into radiomics. Radiol Med 2021; 126: 1296-1311.
[13] Real A, Morais P, Barbosa LCN, Gomes-Fonseca J, Oliveira B, Moreira AHJ and Vilaca JL. A sensorized needle guide for ultrasound assisted breast biopsy. Annu Int Conf IEEE Eng Med Biol Soc 2022; 2022: 865-868.
[14] Secco GM, Gutierrez PA, Secco VL, Chico MJ, Secco RA and Pesce KA. Is breast ultrasound a good alternative to magnetic resonance imaging for evaluating implant integrity? Radiologia (Engl Ed) 2022; 64 Suppl 1: 20-27.
[15] Spak DA, Plaxco JS, Santiago L, Dryden MJ and Dogan BE. BI-RADS(®) fifth edition: a summary of changes. Diagn Interv Imaging 2017; 98: 179-190.
[16] Tagliafico AS, Piana M, Schenone D, Lai R, Massone AM and Houssami N. Overview of radiomics in breast cancer diagnosis and prognostication. Breast 2020; 49: 74-80.
[17] Satake H, Ishigaki S, Ito R and Naganawa S. Radiomics in breast MRI: current progress toward clinical application in the era of artificial intelligence. Radiol Med 2022; 127: 39-56.
[18] Song X, Xu H, Wang X, Liu W, Leng X, Hu Y, Luo Z, Chen Y, Dong C and Ma B. Correction: use of ultrasound imaging Omics in predicting molecular typing and assessing the risk of postoperative recurrence in breast cancer. BMC Womens Health 2024; 24: 456.
[19] Xu M, Zeng S, Li F and Liu G. Utilizing grayscale ultrasound-based radiomics nomogram for preoperative identification of triple negative breast cancer. Radiol Med 2024; 129: 29-37.
[20] Yıldız MS, Goya C and Adin ME. Contribution of Sonoelastography to diagnosis in distinguishing benign and malignant breast masses. J Ultrasound Med 2020; 39: 1395-1403.
[21] Li C, Li J, Tan T, Chen K, Xu Y and Wu R. Application of ultrasonic dual-mode artificially intelligent architecture in assisting radiologists with different diagnostic levels on breast masses classification. Diagn Interv Radiol 2021; 27: 315-322.
[22] Xu J, Zhang L, Wen W, He Y, Wei T, Zheng Y, Pan X, Li Y, Wu Y, Dong F, Zhang H, Cheng W, Xu H, Zhang Y, Bao L, Zhang X, Tang S, Liao J, Luo H, Zhao H, Tian J and Peng Y. Evaluation of standard breast ultrasonography by adding two-dimensional and three-dimensional shear wave elastography: a prospective, multicenter trial. Eur Radiol 2024; 34: 945-956.
[23] Al-Antari MA, Al-Masni MA and Kim TS. Deep learning computer-aided diagnosis for breast lesion in digital mammogram. Adv Exp Med Biol 2020; 1213: 59-72.
[24] Zhang Q, Peng Y, Liu W, Bai J, Zheng J, Yang X and Zhou L. Radiomics based on multimodal mri for the differential diagnosis of benign and malignant breast lesions. J Magn Reson Imaging 2020; 52: 596-607.

[25] Han Y, Lv J, Yu C, Guo Y, Bian Z, Hu Y, Yang L, Chen Y, Du H, Zhao F, Wen W, Shu XO, Xiang Y, Gao YT, Zheng W, Guo H, Liang P, Chen J, Chen Z, Huo D and Li L; China Kadoorie Biobank Collaborative Group. Development and external validation of a breast cancer absolute risk prediction model in Chinese population. Breast Cancer Res 2021; 23: 62.

[26] Niu Z, Tian JW, Ran HT, Ren WD, Chang C, Yuan JJ, Kang CS, Deng YB, Wang H, Luo BM, Guo SL, Zhou Q, Xue ES, Zhan WW, Zhou Q, Li J, Zhou P, Zhang CQ, Chen M, Gu Y, Xu JF, Chen W, Zhang YH, Wang HQ, Li JC, Wang HY and Jiang YX. Risk-predicted dual nomograms consisting of clinical and ultrasound factors for downgrading BI-RADS category 4a breast lesions - a multiple centre study. J Cancer 2021; 12: 292-304.

[27] Qian X, Zhang B, Liu S, Wang Y, Chen X, Liu J, Yang Y, Chen X, Wei Y, Xiao Q, Ma J, Shung KK, Zhou Q, Liu L and Chen Z. A combined ultrasonic B-mode and color Doppler system for the classification of breast masses using neural network. Eur Radiol 2020; 30: 3023-3033.

[28] Youk JH, Kwak JY, Lee E, Son EJ and Kim JA. Grayscale ultrasound radiomic features and shear-wave elastography radiomic features in benign and malignant breast masses. Ultraschall Med 2020; 41: 390-396.

[29] Hong ZL, Chen S, Peng XR, Li JW, Yang JC and Wu SS. Nomograms for prediction of breast cancer in breast imaging reporting and data system (BI-RADS) ultrasound category 4 or 5 lesions: a single-center retrospective study based on radiomics features. Front Oncol 2022; 12: 894476.

[30] Gao J, Han W, Ai Si Mu Tu La DLMT, Hou X, Li ZM and Song T. Value of contrast-enhanced malignancy imaging features in secondary grade diagnosis of BI-RADS-US type 4 breast lesions. Tumori 2021; 107: 424-431.

[31] Du Y, Zha HL, Wang H, Liu XP, Pan JZ, Du LW, Cai MJ, Zong M and Li CY. Ultrasound-based radiomics nomogram for differentiation of triple-negative breast cancer from fibroadenoma. Br J Radiol 2022; 95: 20210598.